On-line measurement of temperature and water vapor in CH_4/air premixed flame using near-infrared diode laser

Bo Tao (陶 波)*, Xisheng Ye (叶锡生), Zhiyun Hu (胡志云), Lirong Zhang (张立荣), and Jingru Liu (刘晶儒)

State Key Laboratory of Laser Interaction with Matter, Northwest Institute of Nuclear Technology, Xi'an 710024, China

**E-mail: nktaobo@yeah.net*

Received April 9, 2010

We establish a single diode laser sensor system to obtain temperature and water concentration in CH_4/air premixed flame. Line-of-sight properties are analyzed, but line-of-sight results are not path average values for temperature measurements. The measurements are performed on a flat burner based on scanned-wavelength direct absorption spectroscopy using two adjacent water lines at 7153.75 and 7154.35 cm^{-1}. Real-time results are acquired using a data acquisition card with a Labview data processing program. The standard uncertainties of the temperature and water concentration measurements are 2.3% and 5.1%, respectively.

OCIS codes: 300.1030, 300.6260, 300.6340.
doi: 10.3788/COL20100811.1098.

Tunable diode laser absorption spectroscopy (TDLAS) has become one of the most powerful tools for combustion diagnostics because of its excellent characteristics such as high spectral resolution, fast response, compact structure, and low cost. Sensor systems based on absorption spectroscopy can offer significant advantages to on-line measurements of multiple flow field parameters, such as temperature, species concentrations, and velocity. Many practical implementations for measuring temperature and species concentrations in engines and detecting atmospheric trace gases have been reported[1−5].

Water is often selected as the absorbing species for temperature sensing because it is a major combustion product. It also has strong rovibrational spectra in the near-infrared region, from which telecommunication lasers and fiber optic technology are well developed[1−3]. In this letter, two adjacent water lines (7153.75 and 7154.35 cm^{-1}) within a single laser scan are selected[6]. We discuss the theory and experimental techniques behind TDLAS, which is essential for resolving the problems in on-line measurements of combustion temperature and water concentration.

The wavelength of distributed feedback (DFB) lasers can be tuned by varying their temperature or injection current. For scanned-wavelength direct absorption spectroscopy, we use linear injection current ramps (sawtooth waveforms at kilohertz rates) to scan the DFB diode laser both in wavelength and intensity, so that the laser wavelength can cross selected absorption lines in every scan. Various combustion parameters can be inferred from the absorption strength and line shapes. A discussion of the advantages and disadvantages of this method compared with others can be found in Ref. [7].

Figure 1 shows a typical detected signal in a direct absorption scan. The laser intensity changes in response to an injection current ramp. A polynomial fit to the non-absorbing wings of the absorption feature is used to extrapolate a zero absorption baseline[7].

According to the Beer-Lambert law, the relationship of transmitted signal I and baseline I_0 can be expressed as[6]

$$I = I_0 \exp[-PXS(T)\phi(\nu)L], \tag{1}$$

where P (atm) is the pressure, X is the mole fraction of absorption species, $S(T)$ ($cm^{-2}\cdot atm^{-1}$) and $\phi(\nu)$ (cm) are the line strength and line shape (generally the Voigt function) of the absorption lines, respectively, and L (cm) is the path length. The signal intensity lies on the sunken depth displayed in Fig. 1, and it can be estimated using

$$d = I_0 - I \approx I_0 PXS(T)\phi(\nu)L. \tag{2}$$

Using Eq. (2) as basis, the signal intensity is determined by laser intensity I_0, absorption coefficient $PXS(T)\phi(\nu)$, and path length L. For a selected line, the signal intensity can be increased using a higher I_0 and a longer L. However, the maximum I_0 in direct absorption measurement is confined by the saturation intensity of the detector, and using a longer L via multiple reflections may introduce more system measurement errors. Therefore, one should choose appropriate parameters to acquire the desired signal intensity.

The combustion temperature is usually obtained by comparing the line strength of two different absorption lines that have different temperature dependence values[7]:

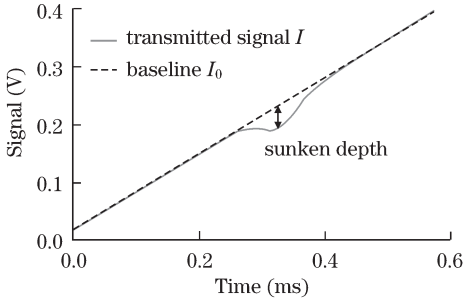

Fig. 1. Typical detected signal in a direct absorption scan (signal intensity lies on the sunken depth).

$$R = \frac{A_1}{A_2} = \frac{\int PXS_1(T)\phi_1(\nu)L\mathrm{d}\nu}{\int PXS_2(T)\phi_2(\nu)L\mathrm{d}\nu} = \frac{S_1(T)}{S_2(T)}. \quad (3)$$

Figure 2 shows the water lines used in this letter. Line 2 consists of two transitions, labeled "a" and "b". Therefore, the total $S(T)$ of line 2 should be a combination of the two transitions. The lower state energy values of the two lines marked "1" and "2" are 1789.04 and 2552.86 cm^{-1}, respectively; the lines have sufficiently different lower state energies to yield high measurement sensitivity. Figure 3 presents the line strength and the line strength ratio as functions of temperature for the two selected water lines. The line strengths are very small at room temperature, ensuring that the absorption from room-temperature water in the measurement path can be neglected in experiments. Line strength ratio R is single-valued with temperature, and the expression of temperature calculation can be acquired using Eq. (3) to fit the R curve:

$$T = -1099.06631/(\ln R + 0.23864). \quad (4)$$

After the temperature is obtained, the mole fraction of the absorbing species can be inferred from either of the two lines[7]:

$$X = \frac{A}{PS(T)L}. \quad (5)$$

We assume that in Eq. (1), the absorbing medium is uniform. For practical combustion fields, the temperature and species concentration are always nonuniform, and the integrated absorbance in Eq. (3) should be expressed as

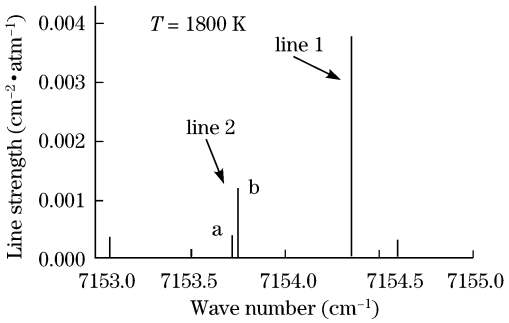

Fig. 2. Water lines utilized in this work (line 2 is composed of two transitions).

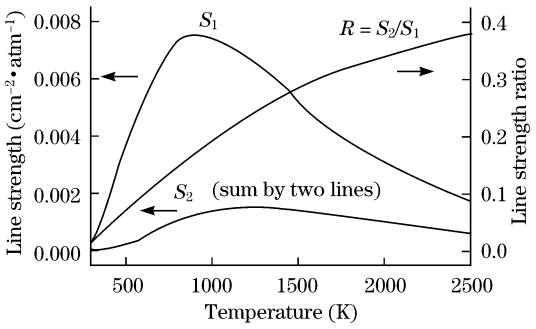

Fig. 3. Line strengths and the line strength ratio as functions of temperature for two selected water lines.

$$A = P\int_0^L X(x)S[T(x)]\mathrm{d}x, \quad (6)$$

where $T(x)$ is the local temperature and $X(x)$ is the local mole fraction of the absorbing species. Mathematically, the measurement result is not the path average value if both parameters are nonuniform. For simplicity, we assume that the measured parameter is nonuniform, and the other, a constant value. In this case, we can acquire the path average value for the measurement of species concentration. However, for temperature measurement, the result is still not the path average value because line strength $S(T)$ is a nonlinear function of temperature.

Figure 4 illustrates the line strengths of two water line pairs (line pair 7153.75 and 7154.35 cm^{-1}; and line pair 7185.60 and 7445.54 cm^{-1}) for two different temperature distributions along the absorption path. The path average temperatures of parabola and trapezoid distributions are 1433 and 1717 K, respectively. The line-of-sight temperatures obtained from Eq. (3) for Figs. 4(a)−(d) are 1266, 1487, 1008, and 1151 K, respectively. Thus, line-of-sight result is related to temperature distribution and line selection. This property may restrict the usefulness of measured data in nonuniform flow fields for TDLAS, and requires further investigation. For the axisymmetric combustion field, the reconstruction method of temperature distribution from line of sight has been described and demonstrated by researchers[8,9].

The sensor system includes a diode laser, data acquisition (DAQ) elements, and optical elements (Fig. 5). Light from the DFB diode laser (NLK1E5EAAA)

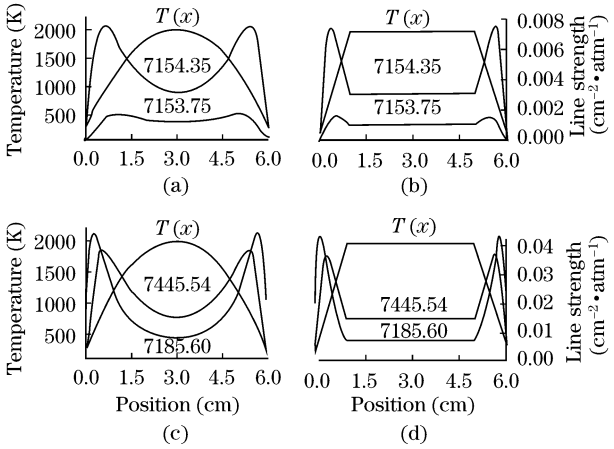

Fig. 4. Line strengths of two water line pairs for two different temperature distributions along the absorption path (both temperature distributions are evaluated at T_{edge}=300 K, T_{core}=2000 K).

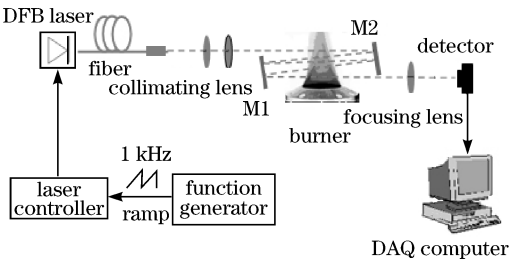

Fig. 5. Schematic of TDLAS measurement system.

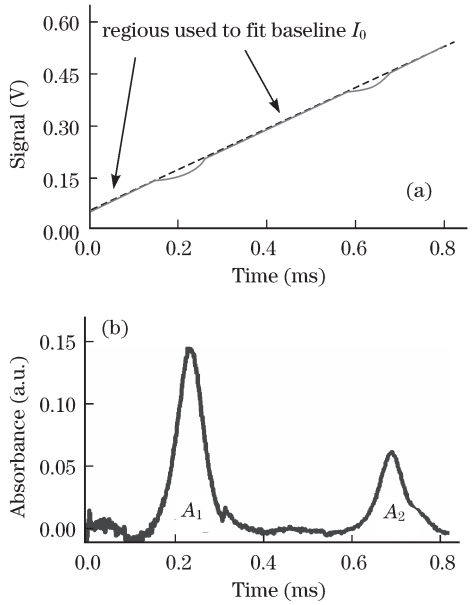

Fig. 6. Typical measured data in each laser scan: (a) schematic of baseline I_0 fitting; (b) schematic of resultant line shapes.

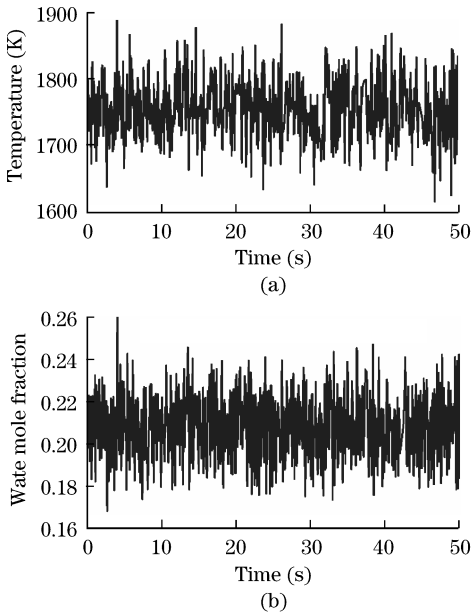

Fig. 7. Measured results as function of time under 1.5-L/min methane flow rate; equivalence ratio is 1. (a) Temperature; (b) water mole fraction inferred from A_1.

emitting near 1397.8 nm (at the same height above the burner surface, and the laser beam is about 2 mm) passes through the CH_4/air premixed flame stabilized on the flat burner (6 cm diameter) five times.

The diode laser is temperature- and current-controlled (ITC502), as well as injection current-tuned (AFG310) across the two absorption transitions. The laser is scanned at 1 kHz across the water line pair to record spectrally resolved absorption line shapes. The transmitted signal is detected (DET50B) and sampled at 1 MHz (PCI4712), corresponding to 1000 points in each laser scan. Incident laser intensity I_0 is determined by fitting the regions outside the absorption lines to a three-

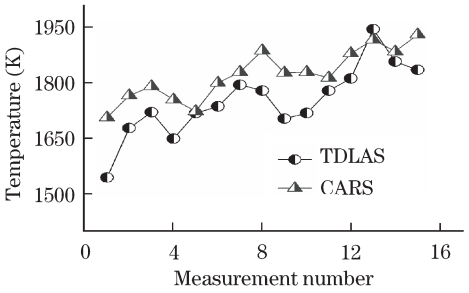

Fig. 8. Comparison of measured temperature with CARS data.

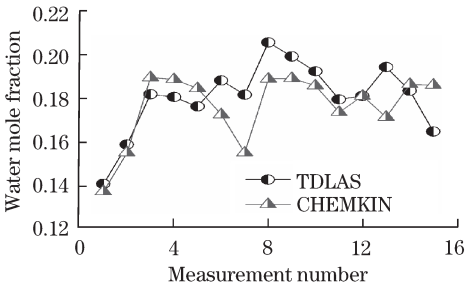

Fig. 9. Comparison of measured water mole fraction with CHEMKIN simulation results.

Table 1. Methane Flow Rate U and Equivalence Ratio Phi for Different Measurements

No.	1	2	3	4	5	6	7	8
U (L/min)	1.1	1.31	1.31	1.31	1.31	1.42	1.73	1.73
Phi	0.7	0.8	1.0	1.1	1.2	0.9	0.8	1.0
No.	9	10	11	12	13	14	15	
U (L/min)	1.73	1.73	1.73	2.05	2.28	2.55	2.55	
Phi	1.1	1.2	1.4	1.3	1.45	1.2	1.39	

order polynomial (Fig. 6(a)). Flame temperature and water mole fraction are inferred from measured integrated areas A_1 and A_2 (Fig. 6(b)) using a Labview data processing program.

Figure 7 illustrates the measured temperature and water mole fraction under a methane flow rate of 1.5 L/min, an equivalence ratio of 1, and a trace of light 1 cm above the burner surface. The real-time readout rate is 12 Hz, restricted to the DAQ card (PCI4712) for its disconnected DAQ. The fluctuation of the measurement results is due to baseline fitting errors, vibration of the flame temperature, beam steering, and uncertainties of instruments. The standard uncertainties of temperature and water mole fraction measurements are 2.3% and 5.1%, respectively, at a temperature of 1750 K and a water mole fraction of 0.2.

Figure 8 shows the comparison of average temperature values with coherent anti-Stokes Raman scattering (CARS) data[10] under different methane flow rates and equivalence ratios (Table 1). The comparison of water mole fraction with CHEMKIN simulation results[10] is presented in Fig. 9. As shown in Fig. 8, the TDLAS results are commonly lower than those of CARS data because the TDLAS results were measured through line of sight, whereas the CARS temperatures were measured in

the core region of the flame. The boundary layer of the flame is not negligible for accurate measurements. The average deviations of temperature and water mole fraction are 3.9% and 2.4%, respectively.

In conclusion, we establish a single diode laser sensor system based on scanned-wavelength direct absorption spectroscopy. A 12-Hz real-time repetition rate of temperature and water mole fraction is achieved. The signal-to-noise ratio is determined by laser intensity, absorption coefficient, and path length. Baseline fitting error is the main source of uncertainty for direct absorption measurements. The primary drawback of this technique is that line-of-sight measurement is used, and the result is closely related to temperature distribution and line selection. This drawback cannot be neglected for temperature measurement, and requires further investigation. A viable method to overcome this problem is to reconstruct temperature distribution from line of sight[8,9].

This work was supported by the State Key Laboratory of Laser Interaction with Matter under Grant No. SKL110905.

References

1. J. T. C. Liu, G. B. Rieker, J. B. Jeffries, M. R. Gruber, C. D. Carter, T. Mathur, and R. K. Hanson, Appl. Opt. **44,** 6701 (2005).
2. H. Li, G. B. Rieker, X. Liu, J. B. Jeffries, and R. K. Hanson, Appl. Opt. **45,** 1052 (2006).
3. H. Li, A. Farooq, J. B. Jeffries, and R. K. Hanson, Appl. Phys. B **89,** 407 (2007).
4. H. Cui, R. Qi, W. Chen, and K. Xu, Chinese J. Lasers (in Chinese) **35,** 1558 (2008).
5. H. Xia, W. Liu, Y. Zhang, R. Kan, M. Wang, Y. He, Y. Cui, J. Ruan, and H. Geng, Chin. Opt. Lett. **6,** 437 (2008).
6. X. Zhou, J. B. Jeffries, and R. K. Hanson, in *Proceedings of 43rd AIAA Aerospace Meeting and Exhibit* AIAA-2005-627 (2005).
7. X. Zhou, "Diode-laser absorption sensors for combustion control" PhD. Thesis (Stanford, University, Stanford, 2005).
8. R. Villarreal and P. L. Varghese, Appl. Opt. **44,** 6786 (2005).
9. A. W. Caswell, S. T. Sanders, and M. J. Chiaverini, in *Proceedings of 41st AIAA/ASME/SAE/ASEE Joint Propulsion Conference and Exhibit* AIAA-2005-4146 (2005).
10. P. Weigend, R. Lückerath, and W. Meier, "Documentation of flat premixed laminar CH_4/air standard flames: temperatures and species concentrations" http://www.dlr.de/VT/Datenarchiv (January 21, 2003).